Energy 118 (2017) 684–691

Contents lists available at ScienceDirect

Energy

journal homepage: www.elsevier.com/locate/energy

Rail coaches with rooftop solar photovoltaic systems: A feasibility study

M. Shravanth Vasisht, G.A. Vashista, J. Srinivasan, Sheela K. Ramasesha*

Divecha Centre for Climate Change, Indian Institute of Science, Bangalore, 560012, India

ARTICLE INFO

Article history:
Received 13 May 2016
Received in revised form
19 September 2016
Accepted 24 October 2016
Available online 1 November 2016

Keywords:
Solar rail coach
Solar train
Photovoltaics
Indian Railways

ABSTRACT

The performance of solar photovoltaic modules mounted on the rooftop of a rail coach of The Indian Railways is reported here. The focus of this experiment was to quantify the reduction in diesel consumption of the end-on generation system that powers the electrical load in the new generation coaches. A coach retrofitted with two flexible solar photovoltaic modules was run at speeds up to 120 km/h by coupling it to three popular trains of south India. Based on the experimental results, the benefits of operating solar rail coaches is projected. It is estimated that one solar rail coach can generate atleast 18 kWh of electricity in a day, leading to an annual diesel saving of 1700 litre. The Indian Railways operates 63,511 coaches and hence, under ideal conditions, can save around 108.5 million litre of diesel annually. This would help to control environmental pollution and mitigate climate change, as it reduces the carbon dioxide emission by 2.9 million tonnes in a year. A statistical model was developed to estimate the power output per unit rooftop area of the coach, to enable The Indian Railways to calculate the benefits of operating solar rail coaches on various routes.

1. Introduction

Few countries have successfully commissioned and operated trains fitted with solar photovoltaic (SPV) system on its rooftop. In Italy, amorphous silicon modules were installed on five passenger coaches, two locomotives and three freight coaches [1]. In 2010, TER-SCNF (Transport Express Régional Société Nationale des Chemins defer Français), the state-owned railway of France tested a Diesel Multiple Unit (DMU) fitted with thin-film CIGS (Copper Indium Gallium Selenide) SPV modules. The SPV system of capacity 990 W_p mounted on the rooftop partially supplied power for electrical lighting system inside the DMU [2]. In 2011, the Indian Railways installed 1 kW_p capacity SPV modules on the rooftop of trains at Pathankot, Punjab, India. The SPV modules power an electrical load of 420 W. Similar attempts were made by Kalka-Simla Mountain Railway, Himachal Pradesh, India to supply power for six LED bulbs of 6 W each [3]. These experiments were done for narrow gauge rail coaches, which run at a maximum speed of 40 km/h. Although the experiments of installing SPV system on trains were successful, no scientific data is available in the public domain for further research and development of Solar Rail Coaches. In 2013, a similar study carried out in Iran, showed that 74% of the power requirement of a coach can be supplied by SPV system during hot months and 25% during cold months. The maximum yield of the SPV system was 63.7 kWh, with an annual reduction of 37 tonnes of CO_2 emission [4]. The Indian Railways being one of the largest railway networks in the world operates around 12,000 trains per day [5]. It is also one of the largest consumers of diesel in the country, with an annual consumption of 2.7 billion litre, which includes locomotion and power supply for coaching stock [6]. Hence, efforts are being made by the Indian Railways to reduce fossil fuel consumption and to adopt eco-friendly technologies [7]. Solar energy can find wide application in the railways sector, especially in tropical countries. The Indian Railways operates 63,511 coaches which include both conventional coaches and Linke Hofmann Busch (LHB) coaches [8]. Most of these coaches remain exposed to sunlight throughout the year. This provides an opportunity for the Indian Railways to explore the possibility of operating Solar Rail Coaches across the country. This would reduce the diesel consumption of End-on Generation (EOG) system which is the power supply for the electrical load in LHB coaches [9]. In this connection, the project 'Solar Rail Coach' was conducted by Divecha Centre for Climate Change, Indian Institute of Science (IISc), Bangalore, in association with Integral Coach Factory (ICF), Chennai. A

* Corresponding author.
E-mail address: sheela@caos.iisc.ernet.in (S.K. Ramasesha).

http://dx.doi.org/10.1016/j.energy.2016.10.103
0360-5442/

LWSCN Coach, which is a LHB Second Class Sleeper Coach, manufactured by ICF was retrofitted with two flexible SPV modules. This coach, named as 'Trial SPV Coach' was run at speeds up to 120 km/h by coupling it to three popular trains of the country. The trials were conducted during the onset of south-west monsoon, so that it would indicate the performance of PV system under low sunshine conditions.

2. The experiment

One of the important constraints considered during the design of the SPV system and module mounting structure (MMS) was the 'Standard Dimensions'. The standard dimensions are declared by Research Design and Standards Organization (RDSO), Ministry of Railways, Govt. of India. According to the guidelines of RDSO, any moving body on the rails must not exceed the Maximum Moving Dimension (MMD). Hence, the SPV modules and MMS were installed such that it doesn't violate the MMD guidelines. The front-view of the roof-arch of the coach is as shown in Fig. 1 (a). Since the roof of the coach was curved, two mono-crystalline flexible SPV modules, each of rating 190 W_p, were used. The modules were mounted along the axis of symmetry as shown in Fig. 1 (b). Since the roof of the coach was corrugated, a flat surface was required to be created along the profile of the roof in order to facilitate stiff and easy mounting of the modules. Hence, a 2 mm thick stainless steel sheet was welded to the crests of corrugates and MMS was mounted on it. MMS was an assembly of Z-frames, rubber sheet, rubber gasket and copper strings. The module was housed inside the module mounting structure. Rubber sheet of the same dimension as the module was placed beneath the module to arrest vibrations of the train. Silica gel was used as an adhesive between the rubber sheet and the SPV modules. Rubber gasket was used to pack the gap between the SPV module and Z-frame. In order to ensure safety of the modules, copper strings fastened across the Z-frame. Hat-shaped conduits were welded to the roof for routing the cables emerging from the modules and these cables were drawn into the coach through the vents provided on the roof for ventilation. A pyranometer was installed along with the MMS to measure the incident solar radiation. A temperature sensor was placed beneath the modules to measure the module temperature. A view of the MMS and modules mounted on the coach are as shown in Fig. 2 (a) and (b), respectively.

An Online Monitoring System (OMS) system consisting of an Embedded Data Acquisition and Control System (EDACS) was developed in order to track and analyse the performance of the SPV system. The OMS was installed inside the coach. The electrical energy generated by the modules was fed to a charge controller which regulated the charging required for the batteries and simultaneously powered the OMS, as shown in Fig. 2 (c). The functions of OMS was to measure, record and display the instantaneous values of parameters such as ambient temperature, module temperature, incident solar radiation, instantaneous power, voltage, current and daily yield. Different sensors were incorporated to measure the above mentioned parameters. The electrical signals from the sensors were directed towards EDACS and OMS. EDACS being an embedded card connected to a computer, the live data generated was being displayed on the screen of the OMS.

To evaluate the performance of the SPV system mounted on the coach, the 'Trial SPV Coach' as shown in Fig. 2 (d), was coupled to three prominent high-speed trains namely, Chennai ↔ Coimbatore Shatabdi Express, Chennai ↔ Mysore Shatabdi Express and Chennai ↔ Bangalore Double Decker Express. The schedule of trials are listed in Table 1. The above-mentioned trains were selected for the dynamic trials (DT) because of high speed of the train, Global

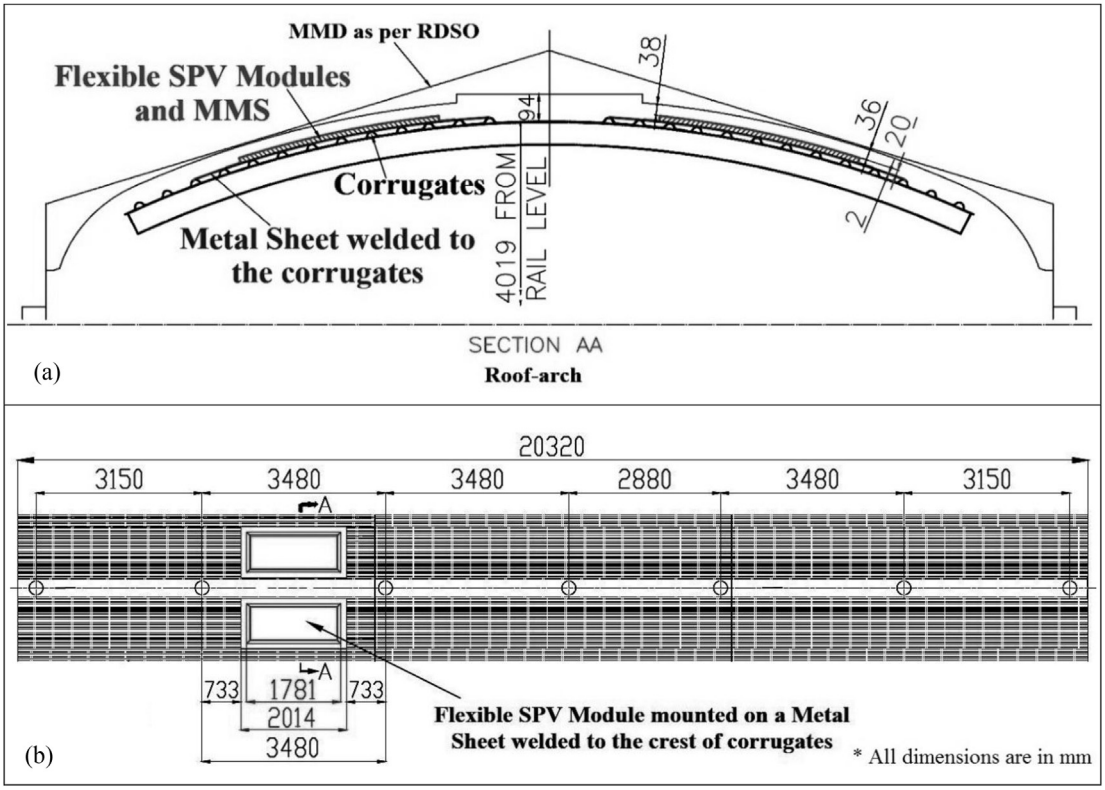

Fig. 1. Layout of Trial SPV Coach (a) Front-view of roof-arch of the coach. The module mounting structure (MMS) does not exceed the maximum moving dimension (MMD) guidelines of Research Design and Standards Organization (RDSO). (b) Top-view of the coach, showing the location of the two flexible SPV modules.

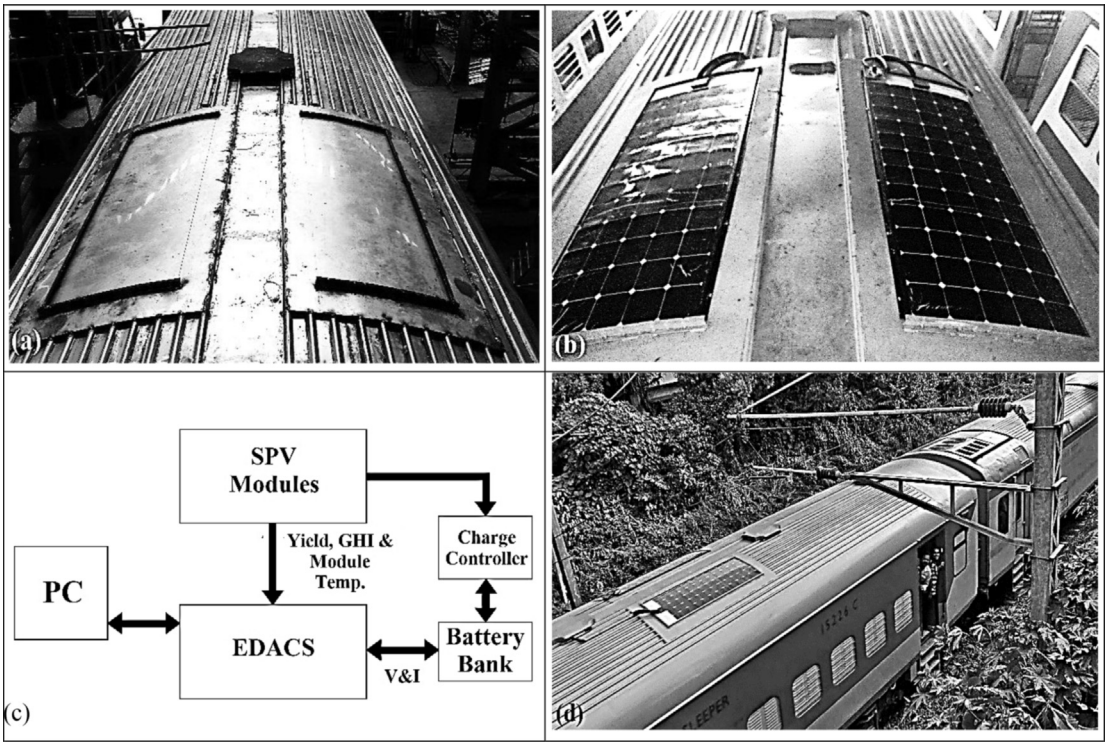

Fig. 2. Trial SPV Coach and Online Monitoring System (OMS). (a) MMS without SPV modules. (b) SPV modules mounted on the coach. (c) Line diagram of OMS. (d) Trial SPV Coach on Trials.

Table 1
Details of trials.

Trial type	Day	Name of the train	Date	Timings (Hours)
Dynamic Trial (DT)	1,2,3	Chennai↔Coimbatore Shatabadi Express	24–26 June 2015	Onward: 07:15–14:15 Return: 15:20–22:15
	4,5,6	Chennai↔Mysore Shatabadi Express	27–29 June 2015	Onward: 06:00–13:00 Return: 14:15–21:25
	7	Chennai↔Bangalore Double Decker Express	01 July 2015	Onward: 07:25–13:10 Return: 14:30–20:35
Static Trial (ST)		Coaching Yard of Chennai	30 June 2015	Dawn to Dusk

Horizontal Irradiance (GHI) and ambient temperatures in the route, duration of transit in sunshine hours (effective sunshine period of 8 h), time of commencement of the transit, compatibility of coupling the coach with the train, compatibility of EOG feeder and safety of coach. The route-map of the trials conducted are as shown in Fig. 3. In addition to DT, it was very important to know the performance of the SPV system when the coach is static. Hence, the coach was parked in the coaching yard on one of the days of the trial period. Since, the static trial (ST) represented the ideal performance of the SPV system, it provided a reference for comparing the results of DT.

3. Results

The data on various performance parameters are presented in this section. Fig. 4 (a) and (b) illustrate the summary of trials conducted. The minimum daily GHI ($I_{d(min)}$), maximum daily GHI ($I_{d(max)}$) and average daily GHI ($I_{d(avg)}$) recorded during dynamic trials (DT) were 4.32 kWh/m^2, 5.64 kWh/m^2 and 4.85 kWh/m^2, respectively. During ST, the daily GHI (I_d) recorded was 4.99 kWh/m^2, which is much lower than $I_{d(max)}$ of DT. This was mainly because of moderately dense clouds uniformly distributed over the city on the day of ST. The maximum daily yield ($Y_{d(max)}$), minimum daily yield ($Y_{d(min)}$) and average daily yield ($Y_{d(avg)}$) of DT were 1.45 kWh, 1.31 kWh and 1.43 kWh, respectively. Although I_d of the day of ST was comparatively lower, the daily yield (Y_d) of ST was 1.81 kWh, which is approximately 20% higher than Y_d of DT. The daily average module efficiency (η_d) of ST and DT were 16.9% and 15%, respectively. Performance ratio (PR), which is the ratio of actual and theoretically possible energy outputs, is one of the most popular metrics for evaluating the efficiency of SPV systems [11]. During ST, the daily PR (PR_d) was 79.5% whereas, during DT, the average PR_d was 71.6%, which is approximately 10% lower than PR_d of ST. For better understanding of the performance of the system, the variations in instantaneous parameters of GHI (I_i), power (P_i), module temperature (T_{mod}) and module efficiency (η_i) are also studied. The comparison of the instantaneous parameters of ST and DT are summarized in Table 2.

3.1. Variation in power and GHI

The performance pattern of the SPV system during DT and ST were different, though the time series plot of GHI curve of the system resembled the bell curve of a typical SPV system exposed to

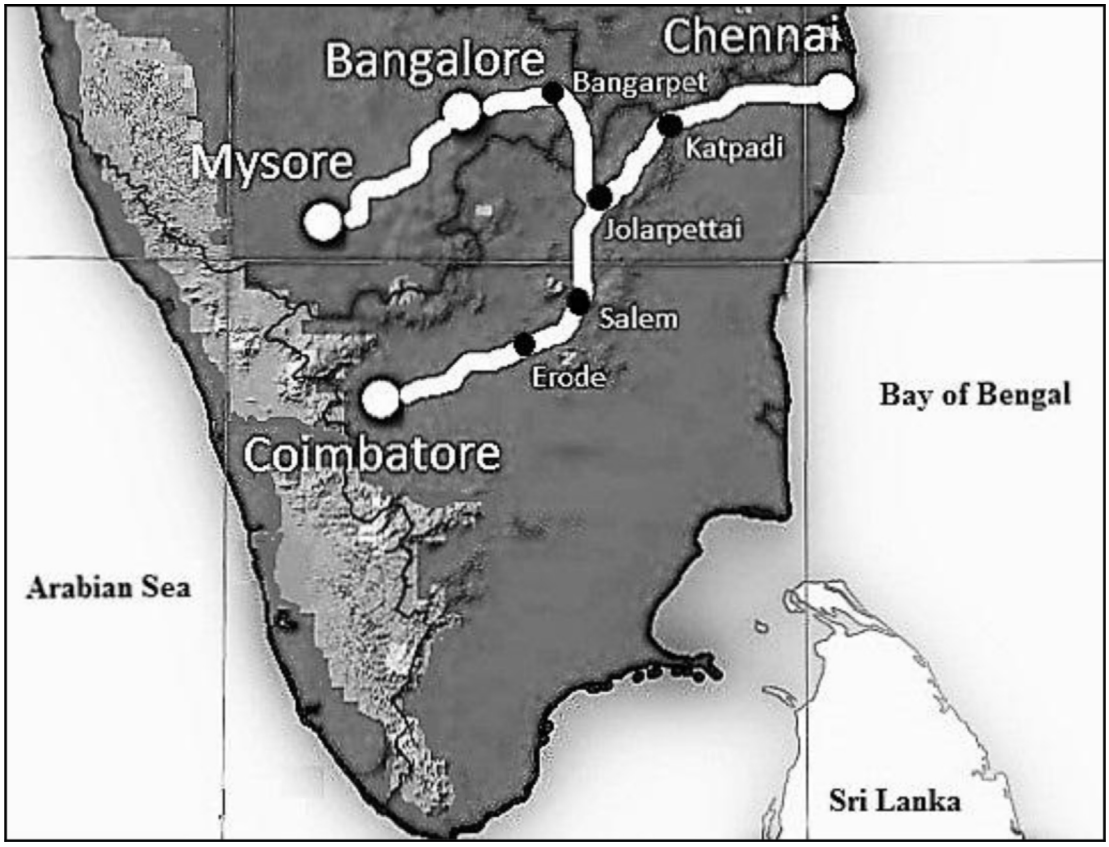

Fig. 3. Route map of trials. The regions shaded in dark and light grey receive an annual average daily GHI, $I_{ad(avg)}$ of 5.5–6.0 kWh/m^2 and 5.0–5.5 kWh/m^2, respectively [10].

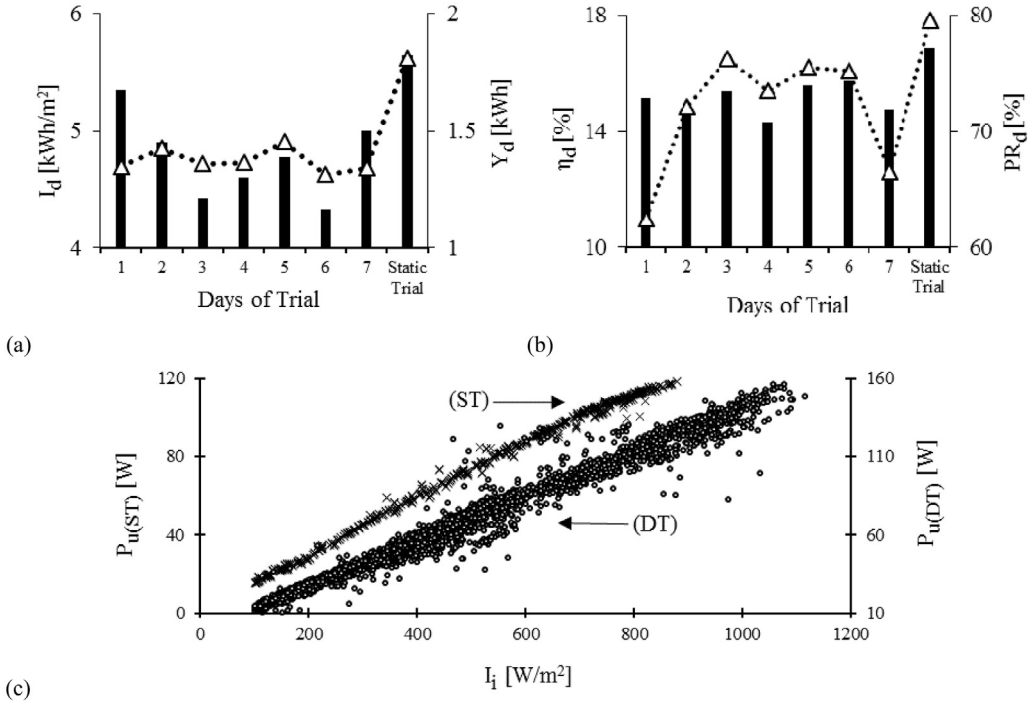

Fig. 4. Summary of Trials: (a) Variation in Y_d and I_d. (b) Variation in daily η_d and PR_d. The bars in (a) and (b) represent I_d and η_d, respectively. The triangles represent Y_d and PR_d, respectively. (c) Variation in P_u corresponding to I_i. Crosses and circles denote $P_{u(ST)}$ and $P_{u(DT)}$, respectively.

Table 2
Comparison of performance parameters of ST and DT.

Parameters	ST	DT
I_i and P_i as a function of time	Smooth bell-shaped curve, with distortions at the peak I_i.	Skewed distribution
T_{mod} as a function of I_i	T_{mod} is directly proportional to I_i. T_{mod} linearly increases by 0.04 °C per unit (1 W/m^2) increase in I_i. T_{mod} has a strong correlation with I_i (R^2 = 98.2%).	I_i influences the variation in T_{mod}. But, the correlation between I_i and T_{mod} is weak (R^2 = 67.2%).
η_i as a function of T_{mod}	$\eta_{i(max)}$ = 20.24% at T_{mod} = 32 °C. For T_{mod}>50 °C, η_i reduces by 13.3% of $\eta_{i(rated)}$, per degree rise in T_{mod}.	$\eta_{i(max)}$ = 21.01% at T_{mod} = 37.3 °C. For T_{mod}>40 °C, η_i reduces by 0.05% of $\eta_{i(rated)}$, per degree rise in T_{mod}. However, the drop in η_i per degree rise in T_{mod} is not as large as static trial.

variety of weather patterns [12]. Fig. 4 (c) shows the variation in P_i per unit area (m^2) (P_u) during ST ($P_{u(ST)}$) and DT ($P_{u(DT)}$) as a function of I_i. It is clear that from Fig. 4 (c) that $P_{u(DT)}$ and $P_{u(ST)}$ have a linear relationship with I_i. However, time series plots of GHI during ST and DT were dissimilar. The comparison of I_i during ST and DT are as shown in Fig. 5 (c). During ST, it was a smooth bell-shaped curve identical to an ideal SPV system. During all the days of DT, the time series plot of I_i was a skewed distribution. This was mainly because of randomly changing orientation of the coach due to curves in the route, variation in angle of tilt due to banking at curves, changing altitudes due to gradients, haphazard shadows due to the landscape and atmospheric uncertainties.

3.2. Influence of module temperature and efficiency

The temperature at the surface of the module is generally higher than the ambient temperature [13]. The variation in T_{mod} corresponding to I_i is as shown in Fig. 5 (a). A strong correlation between T_{mod} and I_i was observed during ST. T_{mod} increased by 0.04 °C per unit (1 W/m^2) increase of I_i. But during DT, the relationship between T_{mod} and I_i were different. The correlation between T_{mod} and I_i were weak. T_{mod} remained as low as 25–32 °C when the coach was in motion and raised upto 55 °C when the coach was at rest. Low T_{mod} during the motion of the train was because of the winds that cooled the module surface. Whereas, when the coach is at rest, T_{mod} increases, unless there is cool wind blowing through its surroundings. Efficiency of SPV modules are affected primarily by T_{mod} [14]. Fig. 5 (b) shows the variation in module efficiency (η_i) for higher T_{mod} for all the days of trials. The drop in η_i during ST was higher for T_{mod}>50 °C than at lower T_{mod}. Hence, T_{mod}>50 °C is considered for the analysis. During ST, for T_{mod}>50 °C, η_i reduced by 13.3% of the rated module efficiency ($\eta_{i(rated)}$), per degree rise in T_{mod}. Whereas during DT, the drop in η_i was as low as 5% per degree rise in T_{mod}. In other words, the rate of decrease in η_i per degree rise in T_{mod} was lower during DT than ST. This is mainly due to the natural cooling which happens when the coach is in motion. However, T_{mod} at maximum module efficiency, ($\eta_{i(max)}$) were dissimilar for ST and DT. During ST, $\eta_{i(max)}$ was 20.24% at a T_{mod} of 32 °C, whereas during DT, $\eta_{i(max)}$ was 21.01%, at T_{mod} of 37.3 °C. This is mainly because the rate of increase in T_{mod} during DT was lower than ST, thus sustaining higher η_i for longer duration.

4. Statistical model for Solar Rail Coaches

It is clear from the above discussions that I_i and T_{mod} are the two dominating factors that exhibit a direct impact on the power output of the system [15]. In specific to this experiment, these two parameters account for various parameters such as cloud-cover, shadows, humidity, wind velocity, ambient temperature [16], orientation [17] and tilt [18] of the modules due to randomly changing directions of transit, speed of transit, etc. A mathematical model for forecasting P_u was derived by carrying out a regression with two variants [19] using the data of 6 days of DT. The resultant equation is,

$$P_c = -3.378 + (0.139453 * I_i) + (0.0927 * T_{mod}) \quad (1)$$

This model was validated for ST and one of the days of DT which were not considered for the regression. The modelled power (P_c) (P_c of DT and ST termed as $P_{c(DT)}$ and $P_{c(ST)}$, respectively) was compared with corresponding P_u, as shown in Fig. 5 (d). Fig. 5 (c) shows the error (X_e) between P_c and P_u. X_e between $P_{c(DT)}$ and P_u is termed as $X_{e(DT)}$ and X_e between $P_{c(ST)}$ and P_u is termed as $X_{e(ST)}$.

The dynamic pattern of module efficiency of a day can be divided into three phases, namely, growth, decay and intermediate phase. Generally, the growth phase lies between the time interval 06:00 to 09:00 h, decay phase between 16:00 to 18:30 h and intermediate phase between 09:00 to 16:00 h. During growth and decay phases, η_i is nearly zero [20] or insignificant due to low I_i, thus leading to high X_e. Whereas during the intermediate phase, η_i is quite high (generally higher than 50% of the rated efficiency of the module), thus leading to low X_e. The variation in $X_{e(ST)}$ and $X_{e(DT)}$ during various instants of the day is as shown in Fig. 5 (c). It is seen that $X_{e(ST)}$ and $X_{e(DT)}$ are lower than 10% for I_i greater than ~320 W/m^2 during ST and ~160 W/m^2 during DT. The average X_e during the growth and decay phases range between 9 and 13% with a maximum of 19.13% for a couple of instances, whereas during intermediate phase, it is 3–4%. This implies that the model provides precise values of power during the intermediate phase of the day than growth and decay phases.

The model can be adopted for estimating the power output and yield of the SPV system by installing the popular sensor device (which is a compact device consisting of sensors to measure I_i and T_{mod}) on one of the coaches of all trains, which would be sufficient to examine the technical feasibility and economic viability of operating Solar Rail Coaches in a specific route.

5. Projections of fossil fuel savings from the present data

The inferences mentioned in the above sections are applicable for operating Solar Rail Coaches in tropical regions, though the performance of the SPV systems in different weather patterns and months of the year vary [21]. The experimental results have been projected based on the experimental data from the two panels to estimate the optimal benefits of Solar Rail Coaches, by considering the feasible rooftop area of a typical LHB coach. Indian solar resource map shows that a major part of the country receives an annual average daily GHI ($I_{ad(avg)}$) of 5.0–6.0 kWh/m^2]. In most of the locations in India, the average number of sunny (clear) days in a year is about 300 [22]. Also, most of the high rail traffic density routes of the Indian Railways lie in these regions. Hence, the mean value of $I_{ad(avg)}$, 5.5 kWh/m^2 is considered for the calculations.

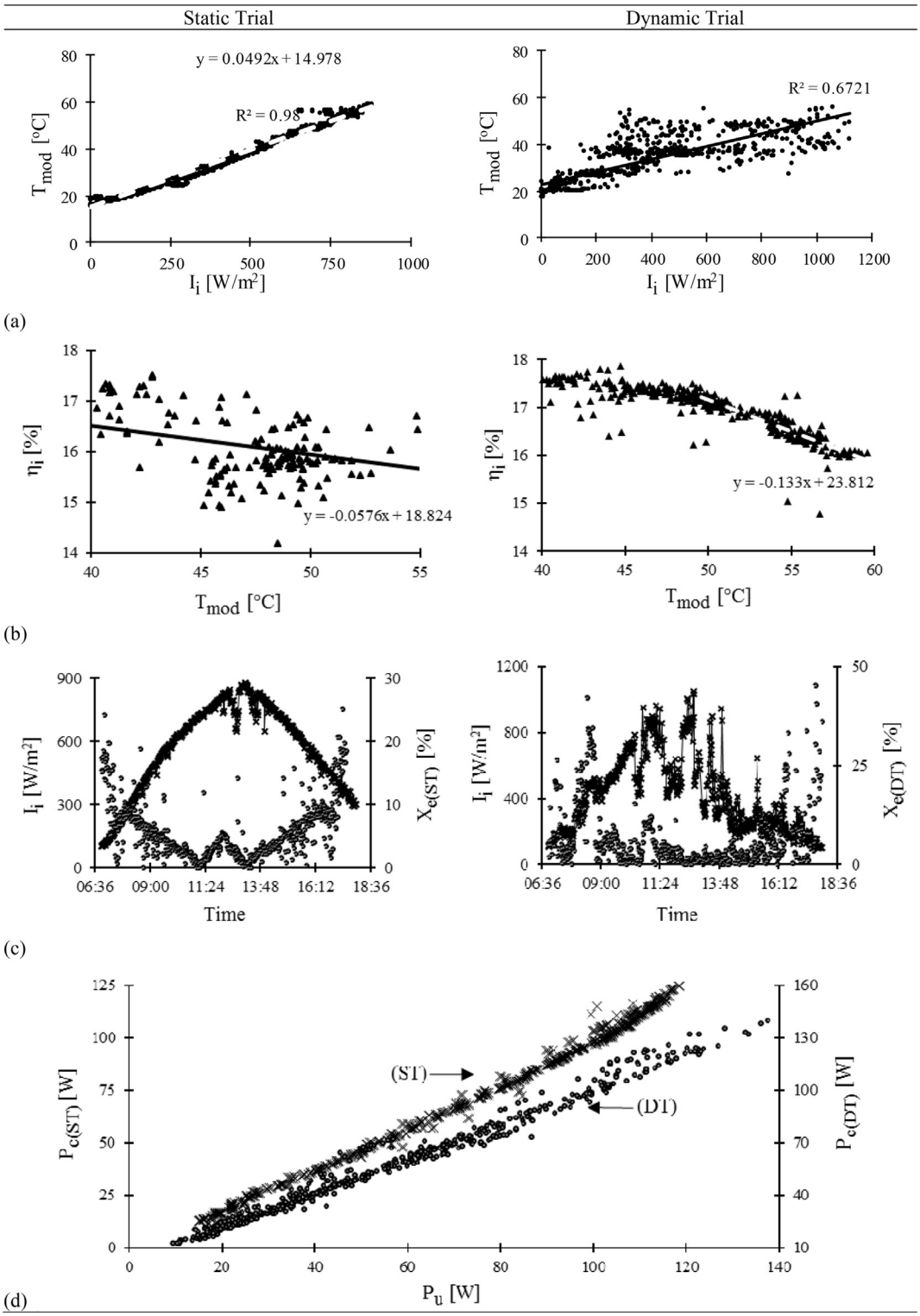

Fig. 5. Performance parameters for ST and DT. (a) T_{mod} as a function of I_i. White broken and black solid line are the straight line fit. (b) Variation in η_i for T_{mod}>40 °C. (c) I_i and error, X_e as a function of time. Circles represent I_i and represent X_e. (d) Comparison of P_c with P_u. Crosses and circles denote $P_{u(ST)}$ and $P_{u(DT)}$, respectively.

Table 3 shows the projection of the benefits of Solar Rail Coach based on the experimental results. Y_d per coach was estimated to be around 18.5–20.2 kWh, thus leading to an approximate daily diesel saving of around 4.6–5.1 litre. Since the passenger service is provided for all days of the year, the coach is assumed to be in operation on all days. Thus, the range of annual yield (Y_a) of a Solar Rail Coach is estimated as 6,820–7,452 kWh under ideal conditions, leading to an annual diesel saving of around 1,708–1,863 litre per coach and annual reduction of around 4.5–4.9 tonne of CO_2 emission. Considering the number of coaches that are operational in the country, the saving of diesel would be significantly large.

Table 3
Projection of the benefits of Solar Rail Coach.

Amount of diesel consumed to generate 1 kWh of electricity [23,24] (litre)				0.25
No. of SPV modules that can be accommodated on one coach				24
Annual average daily GHI, $I_{ad(avg)}$ (kWh/m^2)				5.5
Experimental results [a]				
Parameter	Dynamic trial routes			Static trial
	Chennai ↔ Coimbatore	Chennai ↔ Mysore	Chennai ↔ Bangalore	
Measured Y_d (kWh)	1.376	1.375	1.34	1.811
Measured I_d (kWh/m^2)	4.887	4.567	4.997	5.647
Estimation per coach per day [for $I_{ad(avg)}$]				
Y_d that can be generated from 24 modules (kWh)	18.576	19.872	17.736	–
Diesel savings (litre)	4.644	4.968	4.434	–
Average annual savings per coach				
Net annual yield, Y_a (kWh)			6,820–7,452	
Specific Yield, S_a (kWh/kW$_p$)			4.097–4.477	
Annual diesel savings (litre)			1,708–1,863	
Annual reduction in CO_2 emission (tonne) [25]			4.54–4.95	
No. of Coaches in the Indian Railways[b]			63,511	
Net annual yield, Y_a (kWh)			433,145,020–473,289,372	

[a] Average value of Y_d and I_d measured on each route of the trial.
[b] It is assumed that all the coaches are either on transit or parked in shadow-free region.

5.1. Economic analysis

Economic analysis of a Solar Rail Coach fitted with 'flexible' monocrystalline SPV modules has been carried out, based on the results cost of the experiment. The Solar Rail Coach is estimated to reduce its annual diesel consumption by 1,705 litre, thus leading to a diesel saving of USD 1,237 per year. The initial investment required for retrofitting an SPV system on an existing rail coach is estimated to be USD 12,581 which includes flexible SPV modules, MMS (metal frames, rubber sheets and rubber gaskets as vibration arrestors), power electronic circuits and power transmission cables. The SPV modules have an average life span of 15–20 years, after which the module efficiency reduces to 85% of its rated efficiency. Considering the annual performance depreciation rate of the SPV system as 1%, the Return on Investment (ROI) period is estimated as 10.6 years. However, flexible SPV modules are gaining popularity only in the recent times and is yet to attain commercial viability worldwide. Hence, conventional flat modules can be used in the place of the flexible SPV modules, with suitable modifications in the MMS. This will reduce the initial investment to USD 8914. According to life cycle assessment (LCA) of a SPV system with monocrystalline (flat) SPV modules, the energy payback period is 4.34 years [26]. The ROI period for flat SPV modules after LCA is 9.2 years. However, LCA does not have much significance in this experiment due to the primitiveness of the concept of Solar Rail Coach and hence, it can be precisely carried out after conducting trials of a full-fledged Solar Rail Coach [27]. Thus, ideal ROI period (without considering LCA) would be 7.5 years. ROI period would further reduce if the Solar Rail Coaches are manufactured on a large scale, mainly due to the increase in number of manufacturers of SPV modules, BOS (Balance of System), spare parts, increase in efficiency of the SPV modules, adopting energy efficient devices, technological advancement in energy storage systems and improvement in operational mechanisms. Fig. 6 shows the breakup of initial investment for a Solar Rail Coach consisting of flat SPV modules. Table 4 shows the economic analysis for a Solar Rail Coach and calculation of ROI period.

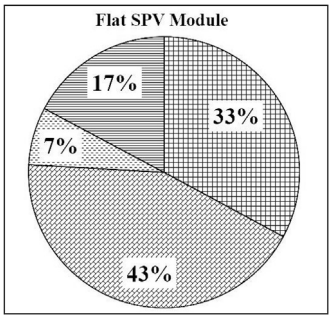

Fig. 6. Break up of Investment for Solar Rail Coach.The sectors shaded in chequers, bricks, dashes and stripes represent SPV module, module mounting structure (MMS), power conditioning unit (PCU) and miscellaneous costs, respectively.

Table 4
Cost Economics of a Solar Rail Coach (in rupees) and Estimation of ROI.

Estimated annual yield (Y_a) from one solar coach (minimum) (kWh)			6,820
Diesel consumption for producing 6,820 kWh of electricity (litre)			1,705
Amount saved on diesel per year (USD) [a] [28]			1,237
Annual Performance Depreciation Rate of SPV System			1%
	Flexible SPV modules	Flat SPV modules	
Price per Watt for SPV modules (USD) [29]	1.04	0.65	
Initial investment for one coach (USD)[b]	12,581	8,914	
ROI period (years)	10.67	7.44	
Life cycle assessment (LCA) (for flat SPV modules)			
Energy consumed to produce a SPV system for one coach (kWh)[c]			29,647
Cost of electricity to produce a SPV system for one coach, considering the tariff of local utility supplying electricity (USD) [30]			2,438
Energy payback period (years)			4.34
ROI period considering LCA			9.17

[a] Currency Exchange Rate: 1 USD = 65.19 INR
[b] Since this project is still at a primitive stage, costs involved in operation, maintenance, periodic overhaul, labour, battery replacement, etc. cannot be estimated.
[c] Energy consumed to produce a SPV system of rating 1 kW$_p$ is 7,278 kWh.

6. Conclusion

Trial SPV Coach, which is a LHB coach retrofitted with two flexible solar photovoltaic modules of 190 W_p, was run by coupling to three prominent high-speed trains of the Indian Railways. The trial was successfully conducted in the Chennai - Coimbatore, Chennai - Mysore and Chennai - Bangalore routes. The period of trials was during the commencement of south-west monsoon and hence, the weather was partly cloudy. The performance evaluation of the SPV system was done by carrying out data acquisition and online monitoring. Different parameters affecting the performance of SPV systems, such as location, module orientation, changing weather conditions, GHI, module temperature and module efficiency have been studied. In addition to the dynamic trials, a static trial was also conducted by keeping the coach stationary in the coaching yard.

The daily yield of the SPV system was around 1.3 kWh with GHI of around 4.8 kWh/m^2. The net yield during the trials was 11.4 kWh. Based on the results of the trials, the annual yield of one Solar Rail Coach is projected. Ideally, one Solar Rail Coach is estimated generate an annual yield ranging between 6,820–7,452 kWh, leading to an annual diesel saving of around 1,708–1,863 litre and reduction in CO_2 emission of around 4.5–4.9 tonne. Minimum period for ROI is estimated as 7.5 years, which would further decrease with increase in number of installations. The Indian Railways operates around 63,511 coaches and deploys around 20 coaches per train. Adopting Solar Rail Coaches for all the trains would provide a minimum generation of 433,145,020 kWh of electricity in a year, leading to a diesel saving of atleast 108,476,788 litre per year and an annual reduction of 288,339 tonne of CO_2 emission. This would also provide an effective solution to mitigate climate change and reduction of oil imports.

The statistical model developed to estimate the power output per unit rooftop area of the coach enables the Indian Railways to evaluate the technical feasibility and economic viability of operating solar rail coaches in different routes of the country, without actually installing SPV modules on the coach. This can be achieved by mounting a compact device which measures irradiance and module temperature. Since the model and its methodology are simple to adopt, it can be customized based on the data of GHI and module temperature obtained during the trials in a specific route. The precision in the forecast model and the realistic benefits of operating solar rail coaches can be established if the trial are carried out for a longer duration and on different routes.

Acknowledgement

We thank Integral Coach Factory (ICF), Southern Railway (SR), South Western Railway (SWR), Indian Railways Organization for Alternate Fuels (IROAF), Ministry of Railways, Government of India, for their support and assistance during the execution of this project.

References

[1] Trentini M. Photovoltaic systems for railways in Italy. In: Tenth E.C. Photovoltaic solar energy conference (vol. 4):826–829, Lisbon, Portugal. http://dx.doi.org/10.1007/978-94-011-3622-8_211.
[2] Disasolar. SME awarded for its innovations for future transportation systems. France. Available at: http://www.idtechex.com/journal/print-articles.asp?articleids=4922 [Accessed 8 August 2015].
[3] RailNews. Solar powered trains in India soon on heritage Kalka-Shimla route. RailNews media ltd. India. Available at: http://www.railnews.co.in/solar-powered-trains-in-india-soon [Accessed 15 August 2015].
[4] Rohollahi E, Abdolzadeh M, Mehrabian MA. Prediction of the power generated by photovoltaic cells fixed on the roof of a moving passenger coach: a case study. J Rail Rapid Transit 2014:1–8. http://dx.doi.org/10.1177/0954409714524749.
[5] Trains. Indian train. 2014-2015. Available at: http://trains.ind.in/indian-train [Accessed 2 September 2015].
[6] Gangwar M, Sharma SM. Evaluating choice of traction option for a sustainable Indian Railways. Transp Res Part D 2014;33:135–45. http://dx.doi.org/10.1016/j.trd.2014.08.025.
[7] Bharath V. India's bio-diesel policy and the current turmoil. Energetica India; 2015. p. 1–4.
[8] Darshana KM, Karnataki K, Shankar G, Ramasesha SK. A practical implementation of energy harvesting, monitoring and analysis system for solar photo voltaic terrestrial vehicles in indian scenarios. In: IEEE international WIE conference on electrical and computer engineering. Dhaka, Bangladesh: IEEE; 2015. p. 542–5. http://dx.doi.org/10.1109/WIECON-ECE.2015.7443989.
[9] Vasisht MS, Vishal C, Srinivasan J, Ramasesha SK. Solar photovoltaic assistance for LHB rail coaches. Curr Sci 2014;107(2):255–9.
[10] National Renewable Energy Laboratory. Updated India solar resource maps. U.S Department of Energy. Available at: http://www.nrel.gov/international/images/india_ghi_annual.jpg [Accessed 6 October 2015].
[11] Jean J, Brown PR, Jaffe RL, Buonassisi T, Bulovic V. Pathways for solar photovoltaics. Energy & Environ Sci 2015;8:1200–19. http://dx.doi.org/10.1039/C4EE04073B.
[12] Su Y, Chan LC, Shu L, Tsui KL. Real-time prediction models for output power and efficiency of grid-connected solar photovoltaic systems. Appl Energy 2012;93:319–26. http://dx.doi.org/10.1016/j.apenergy.2011.12.052.
[13] Jones AD, Underwood CP. A thermal model for photovoltaic systems. Sol Energy 2001;70(4):349–59. http://dx.doi.org/10.1016/S0038-092X(00)00149-3.
[14] Radziemska E. The effect of temperature on the power drop in crystalline silicon solar cells. Renew Energy 2012;28(1):1–12. http://dx.doi.org/10.1016/S0960-1481(02)00015-0.
[15] Vasisht MS, Ramasesha SK. Forecast of solar power a key to power management and environmental protection. Clean Technol Environ Policy 2016. http://dx.doi.org/10.1007/s10098-016-1199-7.
[16] Mekhilef S, Saidur R, Kamalisarvestani M. Effect of dust, humidity and air velocity on efficiency of photovoltaic cells. Renew Sustain Energy Rev 2012;16:2920–5. http://dx.doi.org/10.1016/j.rser.2012.02.012.
[17] Kacira M, Simsek M, Babur Y, Demirkol S. Determining optimum tilt angles and orientations of photovoltaic panels in Sanliurfa, Turkey. Renew Energy 2004;29:1265–75. http://dx.doi.org/10.1016/j.renene.2003.12.014.
[18] Hussein HMS, Ahmad GE, Ghetany HHE. Performance evaluation of photovoltaic modules at different tilt angles and orientations. Energy Convers Manag 2004;45:2441–52. http://dx.doi.org/10.1016/j.enconman.2003.11.013.
[19] Boland J, David M, Lauret P. Short term solar radiation forecasting: island versus continental sites. Energy 2016;113:186–92. http://dx.doi.org/10.1016/j.energy.2016.06.139.
[20] Su Y, Chan LC, Shu L, Tsui KL. Real-time prediction models for output power and efficiency of grid-connected solar photovoltaic systems. Appl Energy 2012;93:319–26. http://dx.doi.org/10.1016/j.apenergy.2011.12.052.
[21] Vasisht MS, Srinivasan J, Ramasesha SK. Performance of solar photovoltaic installations: effect of seasonal variations. Sol Energy 2016;131:39–46. http://dx.doi.org/10.1016/j.solener.2016.02.013.
[22] Sundaram S, Babu JSC. Performance evaluation and validation of 5 MW_p grid connected solar photovoltaic plant in South India. Energy Convers Manag 2015;100:429–39. http://dx.doi.org/10.1016/j.enconman.2015.04.069.
[23] Sharma PK, Sahil, Hari N, Banerjee S, Sharma R. A novel method of generating electricity by setting up turbines over rail locomotives. In: IEEE 6th India international conference on power electronics. Kurukshetra, India: IEEE; 2014. p. 1–5. http://dx.doi.org/10.1109/IICPE.2014.7115794.
[24] RailElectrica. Energy conservation – train lighting and air conditioning. Available at: https://www.railelectrica.com/energy-conservation/energy-conservation-train-lighting-and-air-condtioning [Accessed 21 August 2015].
[25] United States Environmental Protection Agency. Average carbon dioxide emissions resulting from gasoline and diesel fuel, Office of Transportation and Air Quality. Available at: http://www.etieco.com/content-files/EPA%20emissions%20calc%20420f05001.pdf [Accessed 21 October 2015].
[26] Scholten MJMW. Energy payback time and carbon footprint of commercial photovoltaic systems. Sol Energy Mater Sol Cells 2013;119:296–305. http://dx.doi.org/10.1016/j.solmat.2013.08.037.
[27] Kittner N, Gheewala SH, Kamens R. Life cycle considerations for monocrystalline photovoltaics in Thailand. J Sustain Energy & Environ 2012;3(4):143–64.
[28] Indian Oil Corporation Limited. Previous price of diesel. Available at: https://www.iocl.com/products/DieselDomesticPrices.aspx [Accessed 28 October 2015].
[29] Central Electricity Regulatory Commission. Determination of benchmark capital cost norm for solar PV power projects and solar thermal power projects applicable during FY. 2015-16. Available at: http://www.cercind.gov.in/2015/orders/SO17N.pdf [Accessed 23 November 2015].
[30] Ghosh S, Nair A, Krishnan SS. Techno-economic review of rooftop photovoltaic systems: case studies of industrial, residential and off-grid rooftops in Bangalore, Karnataka. Renew Sustain Energy Rev 2015;42:1132–42. http://dx.doi.org/10.1016/j.rser.2014.10.094.